Journal of Computer-Aided Molecular Design, 10 (1996) 589–606
ESCOM

J-CAMD 372

Modelling steric effects in DNA-binding platinum(II)–am(m)ine complexes

Elizabeth Yuriev and John D. Orbell*

Department of Environmental Management, Victoria University of Technology, St. Albans Campus, P.O. Box 14428, MCMC, Melbourne, VIC 8001, Australia

Received 31 December 1995
Accepted 29 July 1996

Keywords: Repulsive energy; Biological indicators; QSAR; Electronic effects; Transport effects

Summary

A repulsive energy strategy has been employed in an attempt to delineate the steric contribution to the biological profile of a variety of platinum–am(m)ine complexes. Thus, relative steric descriptors have been calculated for the amine ligands themselves by the Ligand Repulsive Energy (LRE) methodology. This has been extended to a Complex Repulsive Energy (CRE) strategy whereby the steric requirements of the approach of a metal complex to a site on a target molecule may be evaluated. Specifically, the monodentate approach of a variety of platinum–am(m)ine complexes to the N7 site of a guanine moiety has been considered. The steric descriptors thus obtained have been used in QSAR analysis, resulting in improved regression equations. Attempts have also been made to relate the above descriptors to various biological indicators for given series of complexes. These investigations suggest an optimum steric requirement for minimum toxicity, which could aid in the rational design of such agents.

Introduction

The binding of metal species to nucleic acids is expected to affect a wide range of biological outcomes [1]. More specifically, by binding to DNA some metal species, such as the now familiar cisplatin (*cis*-dichlorodiammineplatinum(II)), show dramatic cytotoxic and antineoplastic activity [2]. Attempts to relate aspects of structure to activity for these compounds, such as the steric influence of the amine carrier ligand(s), have been primarily qualitative in nature [3]. As far as a quantitative treatment is concerned, an extensive literature search revealed a limited number of attempts to correlate the biological activity of platinum–am(m)ine complexes with their structures, four groups being concerned with antitumour activity [4–9] and one with mutagenicity [10]. A search of the MedChem/Biobyte QSAR database [11] revealed an additional two QSARs involving platinum–am(m)ine complexes. These studies, for toxicity only, include cisplatin amongst a number of miscellaneous compounds [12], and a series of substituted dichloro(*o*-phenylenediamine)platinum(II) complexes [13].

In one of the QSAR studies on platinum systems reported in the literature, Abdul-Ahad and Webb [4] have investigated the correlation of standard indicators of biological activity, namely, acute toxicity (pLD_{50}), antitumour potency (pID_{90}) and therapeutic index (log TI), with a variety of structural descriptors. These include a wide range of electronic parameters, and the molecular volume (MV) as a steric parameter. In some cases this has resulted in moderate to strong correlations with a high degree of statistical significance. However, in this study, parameters relating to transport phenomena (e.g. hydrophobicity) have not been taken into account, and the use of MV oversimplifies steric effects since it is a scalar quantity [14]. Steric effects are, in fact, often highly localised and directional.

Tang et al. [9] have used exclusively electronic descriptors to obtain regression equations (having more than three variables), which also show moderate to strong correlation and high statistical significance. Furthermore, these authors report the synthesis of a complex designed to possess the electronic characteristics required by their regression results. This complex is reported to show rela-

*To whom correspondence should be addressed.

TABLE 1
CORRELATION MATRIX FOR THE DESCRIPTORS USED IN REF. 9

	q_{Pt} (e)	$-q_{Cl}$ (e)	$-q_N$ (e)	q_{Am} (e)	ΔE (a.u.)	Q_{Pt-Cl} (e)	Q_{Pt-N} (e)	ΔQ (e)	N_H
q_{Pt}	1								
$-q_{Cl}$	0.4702	1							
$-q_N$	−0.446	0.3272	1						
q_{Am}	−0.1619	0.791	0.6817	1					
ΔE	0.2019	−0.2084	**−0.6416**	−0.3946	1				
Q_{Pt-Cl}	**−0.7859**	**−0.8099**	0.0843	−0.3569	−0.139	1			
Q_{Pt-N}	0.0517	0.742	0.4194	0.7933	−0.0016	−0.5301	1		
ΔQ	−0.3586	**−0.8667**	−0.2702	−0.7186	−0.0535	0.7904	−0.9384	1	
N_H	**−0.7809**	−0.2174	0.5071	0.2975	−0.0583	0.6186	0.1663	0.1317	1

Descriptors: q_{Pt}, $-q_{Cl}$, $-q_N$ and q_{Am} are electronic charges on corresponding atoms and moieties; ΔE is the gap between energies of LUMO and HOMO; Q_{Pt-Cl} and Q_{Pt-N} are overlap populations on corresponding bonds; ΔQ is the difference between the above; N_H is the number of protons on the N atom of the amine.

tively low toxicity and high potency. It is not clear, however, whether this approach is generally applicable.

Simon et al. [5,6] have sought correlations involving hydrophobicity, electronic and steric effects with respect to biological activity. These workers [6] have suggested that the biological activity indicator TI depends predominantly on steric features. For the steric optimisation of TI, a receptor mapping procedure was employed via the minimal steric difference technique, resulting in quite strong and statistically significant correlation results. This approach, however, has certain drawbacks and has received considerable criticism [15,16]. In particular, it should be noted that the parameter used can code both steric and nonsteric factors, and the method does not account for the molecule's three-dimensional structure and conformational flexibility.

All of the researchers referred to so far used either measured physicochemical properties or computed descriptors representing classic QSAR studies (Hansch-type analysis) [17].

A more recent attempt to quantify structure–activity relationships for platinum complexes involves the application of a graph-theoretical method and employs purely topological indices. Thus, Romanowska and co-workers [7,8] have demonstrated the usefulness of molecular topology for structure–activity studies of platinum–am(m)ine complexes. However, even though topological indices generally offer an almost universal means of representing a chemical structure, they usually lack physical or chemical meaning and cannot be extrapolated to other compounds [18,19].

The major weakness of the multiple linear regression (MLR) analysis performed in the above studies, and especially in Ref. 9, is that many of the descriptors are interrelated and the same information is carried by more than one parameter. Such collinearity diminishes the statistical significance, complicates the interpretation of the correlation and may lead to false conclusions and predictions [20]. Collinearity may be diagnosed from a correlation matrix. Thus, correlation matrices have been

TABLE 2
CORRELATION MATRIX FOR THE DESCRIPTORS USED IN REF. 4

	BE (eV)	$EF(P_7)$ (V/Å)	$EF^2(P_7)$ ((V/Å)^2)	$EF(P_9)$ (V/Å)	$E_x(P_3)$ (V/Å)	$E_z(P_9)$ (V/Å)	$F^N(Pt)$ (−e)	MV (Å^3)	$V_2(P_7)$ (V/e)
BE	1								
$EF(P_7)$	0.6187	1							
$EF^2(P_7)$	0.6146	0.9999	1						
$EF(P_9)$	−0.3498	−0.2518	−0.2496	1					
$E_x(P_3)$	0.5656	0.343	0.3364	−0.2655	1				
$E_z(P_9)$	−0.3757	−0.255	−0.2523	**0.9952**	−0.3024	1			
$F^N(Pt)$	−0.0747	−0.1888	−0.191	−0.3437	−0.073	−0.3518	1		
MV	−0.9821	−0.6219	−0.6182	0.3927	−0.4811	0.4128	−0.0037	1	
$V_2(P_7)$	**0.6895**	0.4143	0.4073	−0.0675	0.4642	−0.1137	0.1276	**−0.6625**	1

Descriptors: BE is the molecule binding energy (the difference between the INDO total energy of the molecule and the sum of the energies of the isolated constituent atoms); $EF(P_7)$ and $EF(P_9)$ are the moduli of the electric field at p (receptor point); $E_x(P_3)$ and $E_z(P_9)$ are the components of the electric field at p, calculated by the finite differentiation of the electrostatic potential; $F^N(Pt)$ is the frontier electron density for the nucleophilic attack at Pt; MV is the molecular volume; $V_2(P_7)$ is the energy of polarisation of the complex by a unit point charge placed at p (second-order interaction energy, calculated by an uncoupled Hartree–Fock perturbation procedure). The bold numbers in Tables 1 and 2 depict the correlation coefficients between the descriptors, simultaneously used in the equations obtained in Refs. 4 and 9, which show moderate to strong collinearity (correlation coefficient more than 0.6).

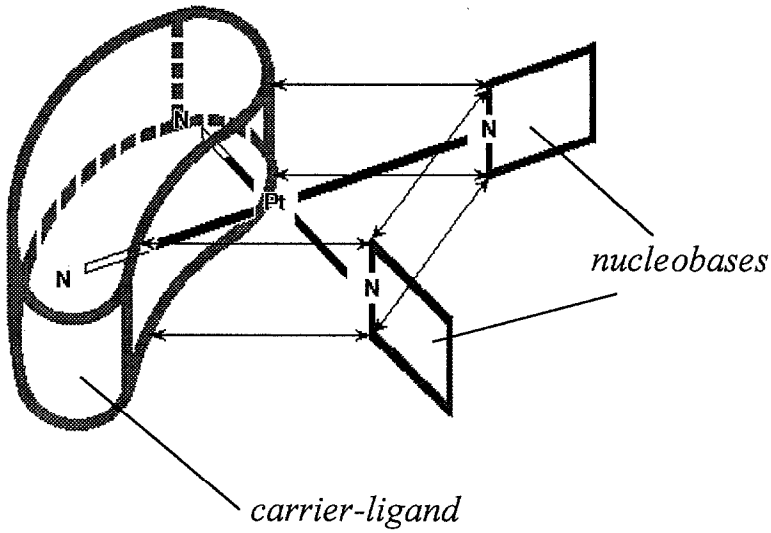

Fig. 1. Potential intramolecular steric interactions in the vicinity of the binding site for a bidentate, metal-mediated, intrastrand cross-linkage. Arrows depict potential steric contacts between the carrier ligand and nucleobases above and below the coordination plane.

reported by some authors [5,7], although we have found it necessary to perform our own computations based on published data [4,9] where this has not been carried out by the authors themselves, Tables 1 and 2.

In summary, research groups studying QSARs of platinum antitumour complexes have investigated the effects of a variety of structural descriptors on biological activity. The highest priority in these studies has been given to electronic descriptors. Hydrophobicity has been less considered, and a quantification of steric effects lags far behind. This could possibly be due to the lack of appropriate steric descriptors as applied to inorganic systems. A number of protocols have been developed in an attempt to quantify such steric effects. These include cone angles Θ [21], solid angles Ω [22], ligand repulsive energy E_r [23], modified vdW energy [24] and stereochemical conventions [25]. However, to our knowledge, there has been no attempt to extend these protocols to QSAR investigations relating to the biological profiles of metal complexes, such as the *cis*-platinum derivatives.

Our analysis of previous work on the QSARs of platinum complexes prompted us to carry out MLR analysis in an attempt to properly account for all three kinds of effects (transport, electronic and steric). In particular, to describe steric effects in platinum complexes, we have applied and extended a recently developed [23] repulsive energy strategy to calculate new steric descriptors. We have also attempted to ascertain the scope of these descriptors both in terms of quantitative structure–activity relationships and particularly with respect to the trends which may be observed in the biological profiles.

Steric effects in platinum systems

All the QSARs discussed above considered the structural features of unbound platinum complexes without a consideration of the structural features of the possible molecular target(s). Today it is widely accepted that DNA is a major intracellular target for cisplatin binding and that its biological activity is manifested through such binding. The multiple binding sites on DNA present the possibility of a diversity of significant steric interactions [25]. Our initial goal is to develop a systematic method for the quantitative assessment of steric effects in platinum(II)–am(m)ine complex/nucleobase systems. For square-planar complexes which may coordinate to nucleobases via a bidentate intrastrand cross-linkage [25], potential intramolecular steric interactions in the immediate

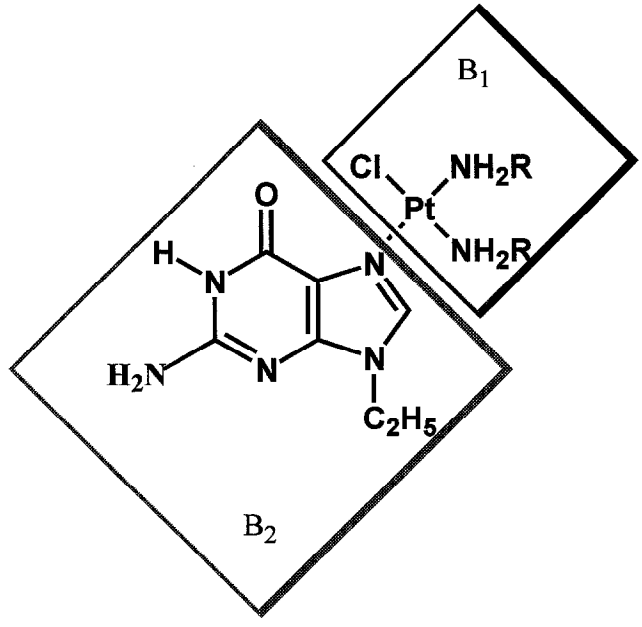

Fig. 2. A representative monoadduct between *cis*-platinum complexes and 9-ethyl guanine.

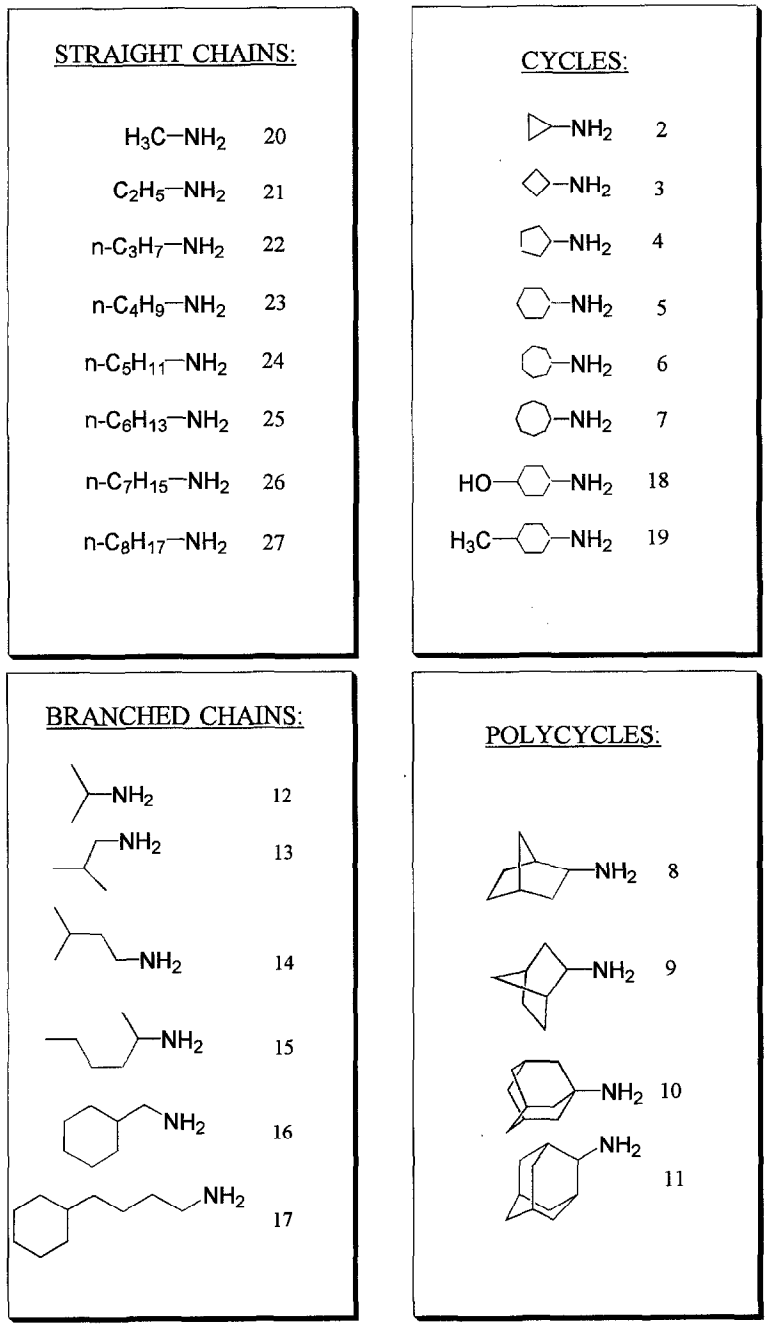

Fig. 3. Amine ligand series employed in this work.

vicinity of the binding site may be characterised schematically as in Fig. 1.

In this work we have directed our initial attention to steric aspects of a potential monodentate precursor [26] represented by the approach of B_1 to B_2, Fig. 2. In choosing this adduct, we assume an initial monodentate attack on the N7 position of the guanine moiety without a replacement of the remaining chloro ligand [27].

It is possible, of course, that the steric demands of both initial and consolidated interactions are relevant to the biological outcomes. In order to investigate the influence of steric properties on biological activity in the above systems, we have adopted two approaches. Firstly, relative quantitative steric descriptors for the ligands (NH_2R) themselves were calculated. Secondly, analogous steric descriptors were developed for the $PtCl(NH_2R)_2$ moiety, B_1 of Fig. 2, with respect to its approach to the nucleobase, B_2.

The first of these two approaches simplifies the calculation of parameters and, in its nature, parallels the use of traditional substituent constants (steric, electronic and hydrophobic) in classical QSAR studies of organic com-

pounds [28]. The second approach (with respect to steric effects only) is more reflective of ligand/receptor modelling in drug/protein studies and may also provide insight into the mechanism of action of the platinum drugs.

Methods

Compounds

Twenty-seven platinum complexes of general formula *cis*-[PtL_2Cl_2], where L is an amine ligand, were chosen as the training set for model building, see Fig. 3. These compounds were selected because their biological profiles have been well characterised [3], Table 3.

Endpoints (dependent variables)

The following biological activity parameters were used for building the model: (i) LD_{50} – acute toxicity, the minimum dose to cause 50% animal death; (ii) ID_{90} – antitumour potency, the minimum dose to cause 90% tumour regression; and (iii) TI – therapeutic index, the measure of the selectivity of the compound as an antitumour agent

TABLE 3
BIOLOGICAL ACTIVITY OF PLATINUM COMPLEXES OF THE TYPE *cis*-[PtL_2Cl_2]

No.	Amine ligand L	pLD_{50}	pID_{90}	log TI
1	Ammonia	1.36	2.27	0.91
2	Cyclopropylamine	0.82	2.22	1.40
3	Cyclobutylamine	0.66	2.15	1.49
4	Cyclopentylamine	–0.04	2.26	2.30
5	Cyclohexylamine	–0.84[a]	1.59	2.43[b]
6	Cycloheptylamine	–0.31	1.81	2.11
7	Cyclooctylamine	–0.10	0.35	0.46
8	*endo*-2-Aminonorbornane	–0.14	1.61	1.74
9	*exo*-2-Aminonorbornane	–0.25[a]	1.19	1.44[b]
10	1-Aminoadamantane	–0.04[a]	–0.04[a]	0.00[b]
11	2-Aminoadamantane	–0.15[a]	–0.15[a]	0.00[b]
12	Isopropylamine	1.06	2.63	1.57
13	Isobutylamine	0.69	1.82	1.13
14	Isoamylamine	–0.42	1.88	2.30
15	2-Aminohexane	–0.19	1.23	1.42
16	Cyclohexylmethylamine	0.74	1.16	0.42
17	1-Amino-4-cyclohexylbutane	0.64	0.64	0.00b
18	4-Aminocyclohexanol	1.35	1.71	0.36
19	4-Methyl-cyclohexylamine	–0.30	–0.38	–0.08[b]
20	Methylamine	1.25	1.43	0.19[a]
21	Ethylamine	1.13	1.47	0.34
22	*n*-Propylamine	1.16	1.50	0.34
23	*n*-Butylamine	0.57	1.61	1.04
24	*n*-Pentylamine	0.68	1.07	0.40
25	*n*-Hexylamine	–0.33	–0.51	–0.15[b]
26	*n*-Heptylamine	–0.26	–0.26	0.00[b]
27	*n*-Octylamine	0.42	0.42	0.00[b]

[a] These values, given in the literature as >, were arbitrarily assigned the minimum quoted value.
[b] These values were calculated from the values for potency and toxicity.

(TI = LD_{50}/ID_{90}). These parameters were measured in the same manner [3] for all the compounds in the series. The units for LD_{50} and ID_{90} were converted from mg/kg to mol/kg.

Descriptors (independent variables)

To model carrier-ligand steric effects in platinum complexes, two descriptors were calculated using the molecular mechanics facilities of HyperChem [29]. These are as follows: (i) LRE – ligand repulsive energy, expressed by the gradient of the van der Waals repulsive energy between the ligand and a $Cr(CO)_5$ fragment, a 'steric probe', to which it binds [23]; and (ii) CRE – complex repulsive energy, expressed by the gradient of the van der Waals repulsive energy between the metal–carrier-ligand moiety and 9-ethylguanine to which it binds, Fig. 2.

Six parameters were chosen to describe the electronic structure of amine ligands in platinum complexes: (i) $q(N)_{PEOE}$ – the partial atomic charge on the amine nitrogen, calculated using the QSAR module of ChemPlus (a set of extension modules to HyperChem), which employs an empirical model built on the partial equalisation of orbital electronegativity (PEOE) method [30]. (ii) $q(N)_{AM1}$ – the partial atomic charge on the amine nitrogen, calculated using the AM1 quantum mechanical method of HyperChem. This method is based on the neglect of diatomic differential overlap (NDDO) approximation [31] and is regarded to be the most accurate semiempirical method of HyperChem and the best method for collecting quantitative information. For this parameter and for $q(N)_{PEOE}$, partial atomic charge/charge density at certain atoms or parts of the molecule can carry information on the reactivity for that part of the molecule [32]. In order to check the suitability of using partial charges in 'amines' for representation in complexes, we calculated nitrogen charges in corresponding Pd complexes using the ZINDO/1 semiempirical method of HyperChem and found a reasonable correlation with the above values. (iii) E_{HOMO} – the energy of the highest occupied molecular orbital of the amine. E_{HOMO} could be a first approximation to the compound's nucleophilicity [33]. (iv) E_{LUMO} – the energy of the lowest unoccupied molecular orbital of the amine. E_{LUMO} could be a first approximation to the compound's electrophilicity [33]. (v) ΔE – the difference in energy levels between E_{HOMO} and E_{LUMO}. (vi) pK_a – the acidity constant of the amine [34–36].

Transport effects were modelled using the octanol/water partition coefficient log P, which is a measure of hydrophobicity. The log P values for the coordinated amine ligands were calculated using the QSAR module of ChemPlus. This calculation is based on an additive function of atomic contributions. Atomic parameters and the functionality for the log P calculation are taken from Ref. 37.

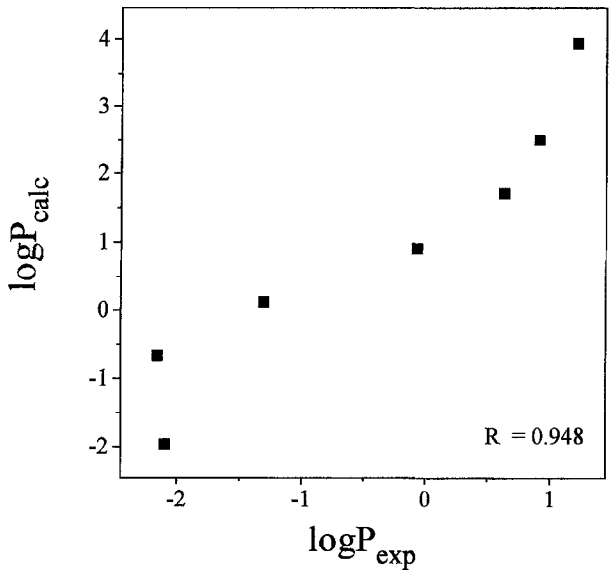

Fig. 4. Plot of calculated log P values (octanol/water) for the coordinated amine ligands in [Pt(NH_2R)$_2$Cl(9-EtG)] versus experimental log P values (chloroform/water) for the complexes themselves, where R represents cycloalkyl substituents. Experimental values are taken from Ref. 3.

To verify that ligand hydrophobicities may be used to model complex transport effects, all available experimental chloroform/water partition coefficients for the complexes themselves were examined for correlation with the theoretical octanol/water partition coefficients for the ligands themselves, Fig. 4. A good correlation was observed for the sample chosen. All of the above descriptors employed in the present work are listed in Table 4. The van der Waals molecular volumes for the amines were calculated using the QSAR module of ChemPlus, see Table 5.

Computational details

All molecular mechanics and quantum mechanics calculations were carried out using the HyperChem molecular modelling and simulation package, versions 3.0 and 4.0 [29], running on AST 486/33 or COMPAQ Pentium 5100 computers.

Semiempirical calculations

The amines of this investigation were geometry optimised utilising the MM+ force field [29]. The conjugate gradient (Polak–Ribiere) algorithm was employed with the termination condition being an rms of less than 0.1 kcal/(Å mol). The quantum-mechanics-derived descriptors used in this investigation were then obtained using AM1 single-point calculations.

TABLE 4
HYDROPHOBICITY, STERIC AND ELECTRONIC DESCRIPTORS

No.	log P	LRE (kcal/mol)	CRE (kcal/mol)	$q(N)_{AM1}$ (e)	$q(N)_{PEOE}$ (e)	E_{LUMO} (eV)	E_{HOMO} (eV)	pK_a	ΔE (eV)
1	–1.96	10.00	4.33	–0.375	–0.339	4.102	–10.530	9.25	14.632
2	–0.67	23.28	8.67	–0.311	–0.325	2.841	–9.568	9.10	12.409
3	0.12	26.57	9.83	–0.326	–0.325	3.424	–9.720	10.64	13.144
4	0.91	28.83	16.45	–0.330	–0.325	3.449	–9.760	10.65	13.209
5	1.71	31.80	21.34	–0.342	–0.325	3.502	–09.594	10.64	13.096
6	2.50	32.87	15.96	–0.345	–0.325	3.479	–09.583	10.67	13.062
7	3.94	37.02	13.59	–0.342	–0.325	3.464	–09.499	10.65	12.963
8	1.37	32.85	11.21	–0.333	–0.324	3.384	–9.672	10.67	13.056
9	1.37	30.17	13.61	–0.330	–0.324	3.367	–9.670	10.67	13.037
10	1.98	42.93	21.73	–0.322	–0.322	3.350	–9.616	10.14	12.966
11	2.62	35.70	17.25	–0.336	–0.324	3.395	–9.603	10.67	12.998
12	0.01	30.60	17.41	–0.344	–0.325	3.492	–9.689	10.67	13.181
13	0.96	33.92	15.83	–0.343	–0.327	3.522	–9.695	10.48	13.217
14	1.61	32.17	16.14	–0.342	–0.327	3.571	–9.617	10.64	13.188
15	2.57	32.66	12.96	–0.344	–0.325	3.488	–9.648	10.63	13.136
16	2.33	24.13	14.16	–0.343	–0.327	3.486	–9.671	10.67	13.157
17	4.57	23.02	15.91	–0.343	–0.327	3.391	–9.730	10.57	13.121
18	–1.34	30.55	19.55	–0.341	–0.325	3.293	–9.707	10.58	13.000
19	2.37	31.62	13.10	–0.342	–0.325	3.493	–9.600	10.67	13.093
20	–1.46	30.00	12.50	–0.340	–0.330	3.714	–9.819	10.64	13.533
21	–0.78	31.00	15.69	–0.342	–0.328	3.579	–9.740	10.64	13.319
22	0.16	31.00	14.15	–0.342	–0.327	3.594	–9.703	10.60	13.297
23	0.95	31.39	21.57	–0.341	–0.327	3.589	–9.692	10.78	13.281
24	1.74	32.26	23.83	–0.341	–0.327	3.575	–9.695	10.71	13.270
25	2.54	31.68	19.07	–0.341	–0.327	3.565	–9.697	10.63	13.262
26	3.33	31.62	16.07	–0.341	–0.327	3.554	–9.696	10.67	13.250
27	4.12	33.99	27.63	–0.342	–0.327	3.544	–9.699	10.65	13.243

TABLE 5
VAN DER WAALS MOLECULAR VOLUMES OF AMINES

No.	MV (Å^3)	No.	MV (Å^3)	No.	MV (Å^3)
1	22	**10**	159	**19**	131
2	67	**11**	159	**20**	40
3	82	**12**	74	**21**	57
4	97	**13**	91	**22**	74
5	114	**14**	108	**23**	91
6	130	**15**	125	**24**	108
7	147	**16**	130	**25**	125
8	121	**17**	182	**26**	142
9	121	**18**	123	**27**	159

Molecular mechanics

The structures of the chromium series, $Cr(CO)_5L$, used in the LRE calculations were optimised using the MM+ force field modified by adding the parameters presented in Table 6, in addition to those derived by Brown and co-workers [23]. For the CRE calculations the structures of the platinum series, $[PtL_2(9\text{-EtG})Cl]$, were optimised using the AMBER force field modified by adding parameters developed for the modelling of monoadducts (Table 6), in addition to those derived by Yao et al. [38] for the modelling of bisadducts.

As the systems under study in this work present an appreciable conformational flexibility, two conformational search procedures for a global energy minimum were implemented, namely quenched dynamics followed by simulated annealing, and Monte Carlo conformational search. Both procedures resulted in almost identical final structures. Preference was given to the latter procedure because of its computational efficiency. A more detailed description of force field development, optimisation conditions, global energy minimum conformational searching and a comparison of molecular mechanics simulation results with X-ray analyses will be published separately.

Repulsive energy strategy

To accommodate alternative software [29], the procedure as described in Ref. 23 was slightly modified. Information on these modifications is available on request. Using Ref. 23 as a control, identical outcomes were established for the LRE values calculated for selected amine ligands. The general strategy for the calculation of both LRE and CRE is similar and may be described as follows:

(1) Obtain the lowest energy structure for the complex ($Cr(CO)_5L$ or $[PtL_2(9\text{-EtG})Cl]$ for LRE or CRE calculation, respectively, where L is an amine ligand).

TABLE 6
FORCE FIELD PARAMETERS

	r_0 (Å)	k_r (mdyn/Å)	k_r (kcal/(mol Å^2))[a]	Θ_0 (°)	k_Θ (kcal/(mol rad^2))[a]	ϕ_0 (°)	n	V/2 (kcal/mol)[a]	r* (Å)	ε (kcal/mol)
MM+ bond stretch parameters										
Cr-N(sp^3)	2.14	2.625[b]								
AMBER parameters[c]										
Bond stretch parameters										
PT-CL	2.305[d]		366							
Angle bend parameters										
NB-PT-CL				90	42					
N3C-PT-CL				90	42					
N3T-PT-CL				180	42					
PT-N3-CT				109.47[d]	20					
PT-N3-H3				109.47[d]	20					
CB-NB-CK				106[e]	70					
Torsional parameters										
CK-NB-PT-CL						90	2	0.25		
CB-NB-PT-CL						90	2	0.25		
Nonbonded parameters[f]										
Atom type PT									1.75	0.1

[a] These force constants were set by analogy to those developed in Ref. 38.
[b] This force constant was set larger than that in Ref. 23 to adjust HyperChem for the inclusion of 1,3-metal centred contacts into the vdW interactions (J. Polowin, personal communication).
[c] Two new atom types were used: N3C (a Pt-bound ligand nitrogen, cis to Cl) and N3T (a Pt-bound ligand nitrogen, trans to Cl). All relevant parameters involving the N3 atom types available in the HyperChem AMBER force field were duplicated for these two atom types.
[d] These values were chosen upon analysis of available crystal structures.
[e] This angle value was found to give a better match to crystal structure data [27] than the angle value developed in Ref. 38.
[f] These parameters were set as suggested in Ref. 29.

(2) For a given complex, vary r_{Me-N} by ± 0.08 Å, with all the other internal coordinates frozen, to create a set of structures.

(3) Using the nonbonded parameters of a modified MM+ force field for both $Cr(CO)_5L$ and $[PtL_2(9\text{-EtG})Cl]$ series, compute the repulsive portion of E_{vdW} for each structure in the above set according to

$$E_{vdW}(rep) = \sum D_0 \exp\left[\gamma \frac{r_0 - r}{r_0}\right] \quad (1)$$

(4) Calculate the repulsive energy according to

$$E_R = -r_e \left[\partial E_{vdW}(rep)/\partial r_{Me-N}\right] \quad (2)$$

where D_0 represents the potential well depth, γ is a scaling factor (typically 12.5), r is the interatomic distance in the energy-minimised structure and r_0 is the unstrained interatomic distance. r_{Me-N} represents a varied metal-to-nitrogen distance (the Cr-N distance in $Cr(CO)_5$ complexes and the Pt-N7 distance in $[PtL_2(9\text{-EtG})Cl]$) and r_e is the metal-to-nitrogen distance in the energy-minimised structure.

Data analysis

Data analysis was performed using the SPSS [39] and SCAN [40] software packages. Multiple linear regression analysis was carried out in two ways, *stepwise* and *enter*.

Stepwise regression analysis

This procedure involves a computerised selection of the best single variable and then considers the remaining variables one at a time until the best two (or more)-variable equation is arrived at. A variable enters the equation only if the significance probability, p, associated with the F-test (which tests the hypothesis that the correlation coefficient equals zero) is less than 0.05 (95% confidence level). The process continues until the addition of a variable is not justified by the 'F-statistic'.

Enter regression analysis

This alternative/complementary approach involves the computation of multiple regression with a fixed set of variables. Because situations are possible where significant variables show up only in a certain combination of two or more [17], both of the above approaches were employed as follows. Firstly, stepwise-MLR was applied to pick up the 'best' equations with one or more variables. Secondly, enter-MLR was carried out on intuitively chosen variables to see if an improvement with respect to correlation strength and statistical significance occurs. To avoid generating meaningless regression results, endpoint versus descriptor plots were checked for clusters, outliers, parabolic behaviour, etc., prior to the regression analysis.

The following interpretation of correlation coefficients was implemented: 0–0.2, very weak; 0.2–0.4, weak; 0.4–0.7, moderate; 0.7–0.9, strong; 0.9–1, very strong. The following criteria were implemented for the choice of the best model [41]: to be useful the model should be able to explain the majority of biological variance, i.e. R^2 should be greater than 0.5; an increase of 0.05 to 0.1 in the value of the correlation coefficient R and a similar decrease in the value of the standard error s are estimates of a significant change. The cross-validated variance R^2_{cv} is a measure of model predictive power (the leave-one-out procedure was used).

Results and Discussion

In this study we adopt the assumption that all of the platinum complexes referred to target the N7 position of guanine. Their individual biological profiles are attributed to the transport, steric and electronic consequences resulting from modification of the amine ligand(s). Thus, the cisplatin analogues chosen for this study feature standard modifications which are expected to influence biological outcomes [28].

LRE as a steric descriptor

It was mentioned previously (vide infra) that the use of MV as a steric descriptor oversimplifies steric effects since MV is a scalar quantity. In the context of this work, there is another consideration which must be taken into account. Not surprisingly, for the ligands of this study MV correlates very well with hydrophobicity as shown in Fig. 5a ($R = 0.95$). Hence, MV carries with it an undesirable amount of transport information. On the other hand, the steric descriptor LRE is much less correlated with hydrophobicity as shown in Fig. 5b ($R = 0.44$). It should also be noted that when the sole ligand of the series which may be considered hydrophilic, i.e. NH_3 (circled data point), is omitted from the regression, the correlation coefficient drops to $R = 0.22$. Indeed, the horizontal array of Fig. 5b suggests a high degree of separation of transport and steric effects, and bolsters our confidence in LRE as a steric descriptor.

CRE as a steric descriptor

Employing a rigid symmetrical steric probe such as $Cr(CO)_5$, the LRE method allows the relative repulsive energies of a series of ligands to be assessed and to be applied to other systems [42]. On the other hand, the CRE method developed in this work is tailored to a particular scenario. Thus, we consider the monodentate interaction of a platinum complex, namely $Pt(NH_2R)_2Cl^+$, with the N7 position of a guanine moiety, Fig. 2. If guanine is considered as the steric probe, since it is obviously not spherically symmetrical with respect to the direction of approach, it is first necessary for the approach to be

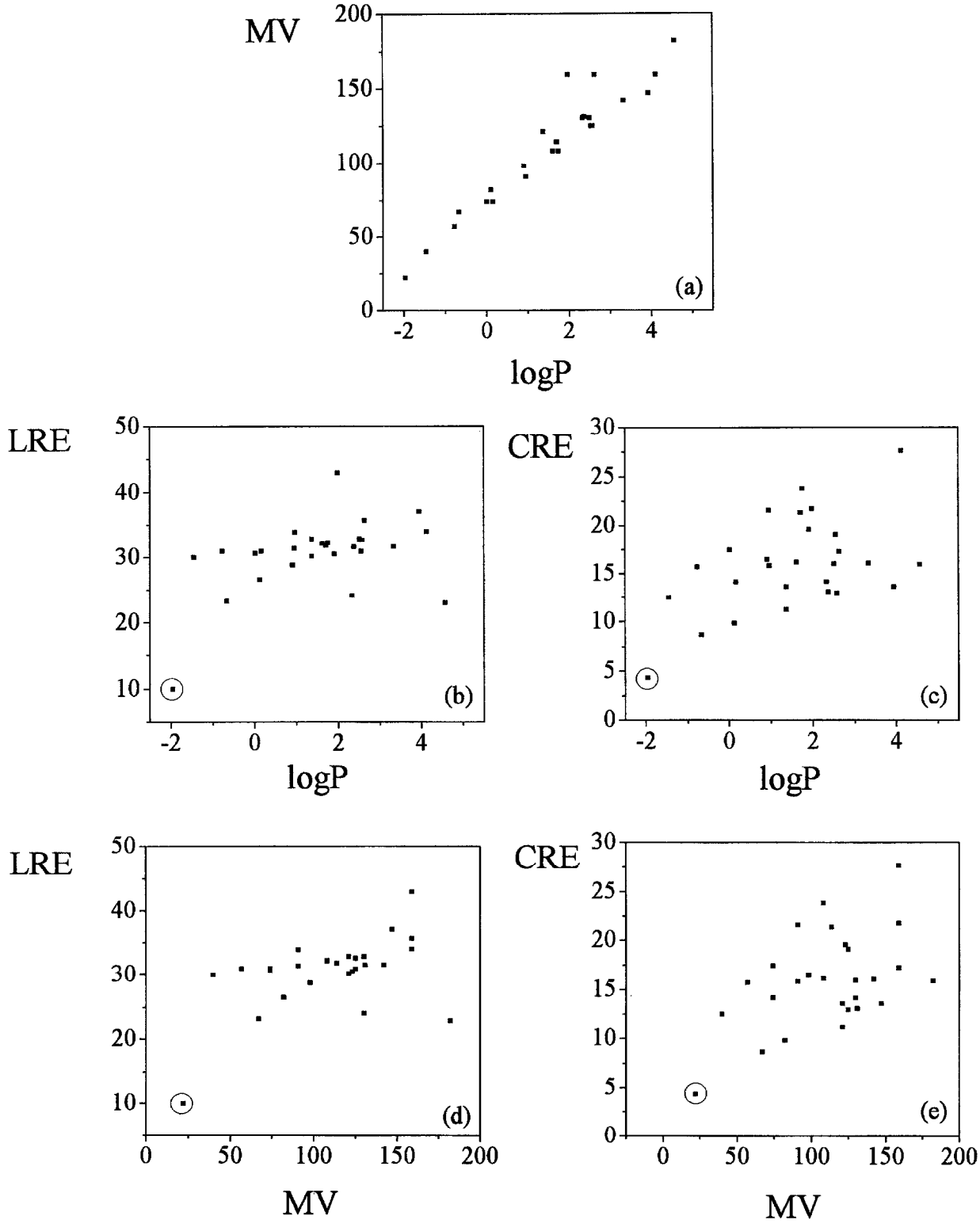

Fig. 5. Relationships between steric and transport descriptors.

optimised. This may be approximated by a global minimum conformation search for the postulated adduct. During this procedure, the orientation of the nucleobase to the coordination plane, the orientation of the 9-ethyl substituent relative to the nucleobase as well as the conformation of the carrier ligand are varied. Thus, the CRE values obtained represent relative measures of steric characteristics presented by each $Pt(NH_2R)_2Cl^+$ moiety towards a specific DNA constituent.

Like LRE, CRE correlates poorly with hydrophobicity

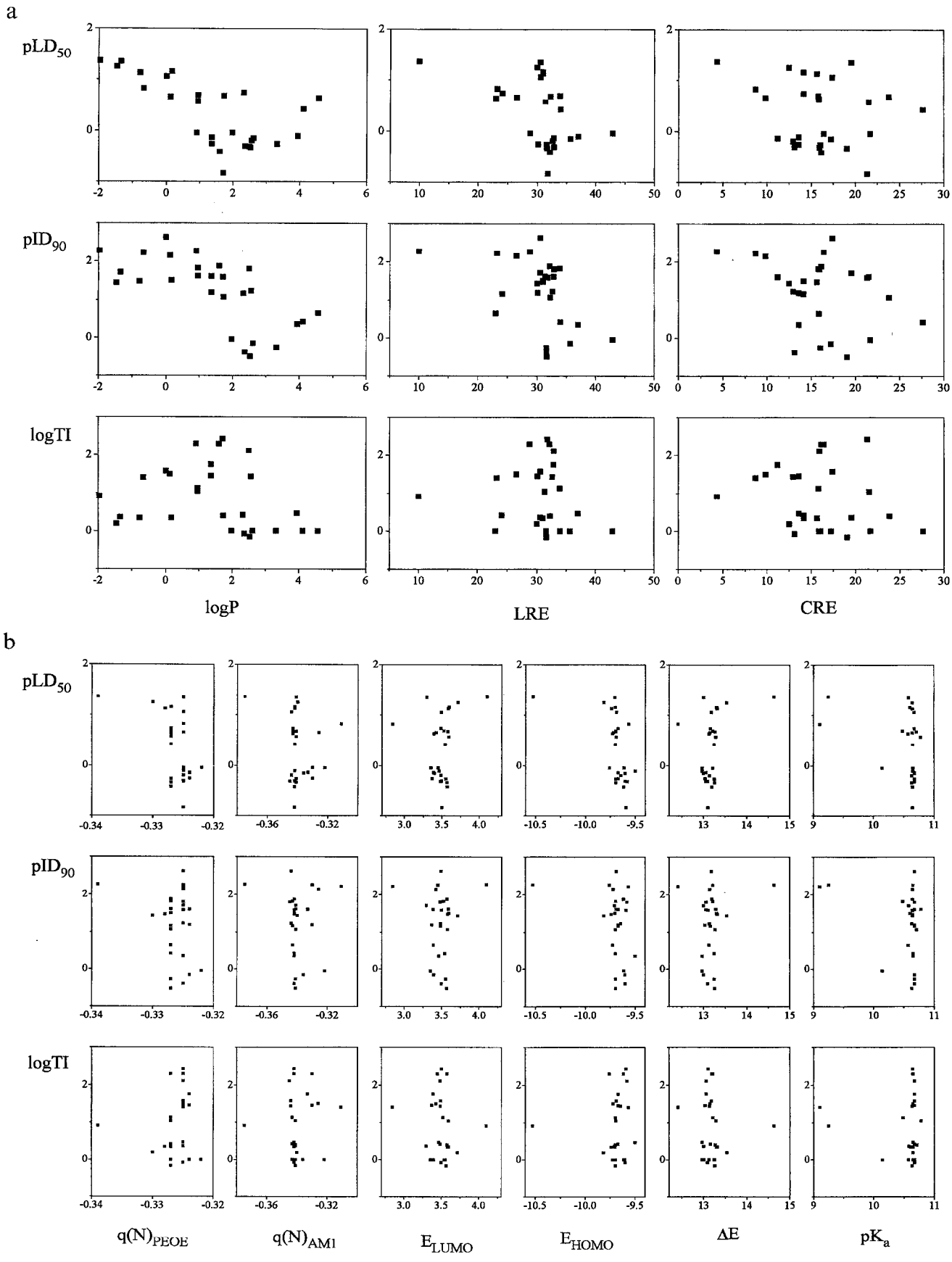

Fig. 6. Endpoints versus (a) transport and steric descriptors, and (b) electronic descriptors.

TABLE 7
CORRELATION MATRIX FOR THE VARIABLES USED FOR THE MLR ANALYSIS

	log P	LRE (kcal/mol)	CRE (kcal/mol)	pK_a	$q(N)_{PEOE}$ (e)	$q(N)_{AM1}$ (e)	E_{LUMO} (eV)	E_{HOMO} (eV)	ΔE (eV)
log P	1								
LRE	0.419	1							
CRE	0.418	0.605	1						
pK_a	0.428	0.560	0.499	1					
$q(N)_{PEOE}$	0.401	**0.739**	0.372	0.434	1				
$q(N)_{AM1}$	0.170	0.547	0.233	0.190	**0.845**	1			
E_{LUMO}	−0.144	−0.290	−0.064	0.114	**−0.761**	**−0.848**	1		
E_{HOMO}	0.495	**0.748**	0.413	0.493	**0.897**	**0.798**	**−0.698**	1	
ΔE	−0.337	−0.551	−0.249	−0.189	**−0.896**	**−0.894**	**0.929**	**−0.913**	1

(R = 0.5; with the NH_3 data point removed, R = 0.37), Fig. 5c. The slightly higher correlation for CRE compared to LRE is perhaps due to a shift of emphasis away from the symmetrical region around the donor nitrogen onto the bulk of the carrier ligand which may impinge on the opposing nucleobase.

Not unexpectedly, given the close relationship between hydrophobicity and MV for these ligands (Fig. 5a), the correlation of both LRE and CRE with MV is also poor (Figs. 5d and e) (R = 0.51 and 0.49 for LRE and CRE, respectively). With the NH_3 data point removed, R = 0.29 and 0.49 for LRE and CRE, respectively.

For the ligands considered here, it is expected that a larger molecular volume will be associated with a more flexible molecule. In a platinum complex, ligand flexibility is expected to increase the likelihood of steric contacts with an opposing nucleobase. The question of the rigidity of steric bulk will be addressed in future studies.

The above considerations of LRE and CRE have the potential to provide insights into the distribution of sterically significant bulk on the carrier ligand. This may be of particular importance in the design of systems whereby sterically restrictive carrier ligands are employed in an attempt to enforce or manipulate a particular orientation of nucleobase(s) such as 'head-to-tail' or 'head-to-head' [43].

Analysis of simple endpoint–descriptor relationships

For all the series combined (Fig. 3), an analysis of the relationship between the biological activity and the structural descriptors (Figs. 6a and b) reveals the following trends:

(1) Not unexpectedly [28], the biological activity suggests a parabolic dependence on log P, especially the acute toxicity and, to a lesser degree, the therapeutic index, Fig. 6a. This observation prompted us to include the quadratic term $\log^2 P$ into the MLR analysis.

(2) With respect to LRE and CRE, the biological activities do not reveal any obvious correlations, Fig. 6a.

TABLE 8
RESULTS OF THE STEPWISE AND ENTER MLR ANALYSES

Equation	n	s	R	F(p)	R^2_{cv}
Stepwise					
$pLD_{50} = 0.08 \log^2 P - 0.45 \log P + 0.56$	27	0.42	0.78	19.10(0.0000)	0.51
$pID_{90} = -0.35 \log P + 1.69$	27	0.68	0.67	19.85(0.0002)	0.36
$\log TI = -0.07 \log^2 P + 1.20$	27	0.77	0.44	6.14(0.0204)	0.11
Enter with LRE as steric parameter					
$pLD_{50} = 0.09 \log^2 P - 0.48 \log P - 0.01$ LRE $+ 0.27\ pK_a - 1.96$	27	0.42	0.80	10.49(0.0001)	0.53
$pID_{90} =$	27	0.66	0.72	8.48(0.0006)	0.42
$0.34 \log P - 0.067$ LRE $+ 1.8\ E_{HOMO} + 21$*	27	0.68	0.70	7.46(0.0012)	0.31
$-0.31 \log P - 0.037$ LRE $- 0.63\ E_{LUMO} + 5.0$					
$\log TI =$	27	0.74	0.59	2.92(0.044)	0.10
$-0.13 \log^2 P + 0.27 \log P - 0.07$ LRE $+ 72\ q(N)_{PEOE} + 27$*	27	0.75	0.57	2.72(0.056)	0.14
$-0.15 \log^2 P + 0.32 \log P - 0.05$ LRE $- 0.42\ E_{LUMO} + 4.2$					
Enter with CRE as steric parameter					
$pLD_{50} = 0.095 \log^2 P - 0.51 \log P - 0.02$ CRE $+ 0.14\ pK_a - 0.58$	27	0.42	0.80	19.10(0.0000)	0.52
$pID_{90} = -0.35 \log P - 0.02$ CRE $+ 0.33\ E_{HOMO} + 5.19$	27	0.71	0.67	19.85(0.0002)	0.33
$\log TI = -0.12 \log^2 P + 0.26 \log P - 0.04$ CRE $- 0.11\ pK_a + 2.8$	27	0.77	0.54	6.14(0.0204)	0.10

Equations marked with an asterisk have a strong degree of collinearity (see Table 7), so the second equation is provided.

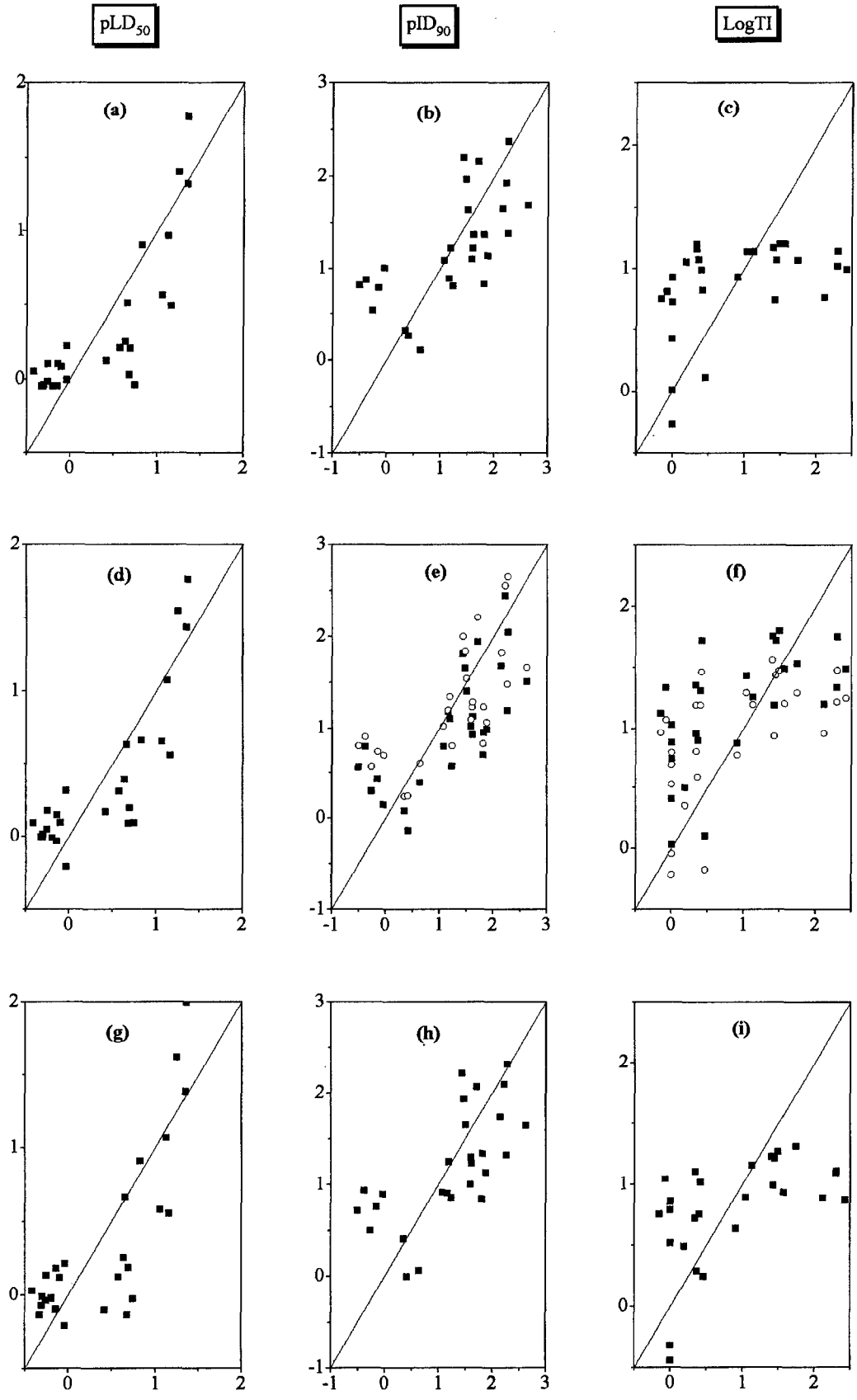

Fig. 7. Plots of calculated versus observed values for the biological activity indicators. Data in plots a, b and c: calculated according to equations from Table 8, upper part; d, e and f: equations from Table 8, middle part; g, h and i: equations from Table 8, lower part. In plots e and f, ■ represents equations marked with an asterisk and o represents second equations provided for pID_{90} and log TI.

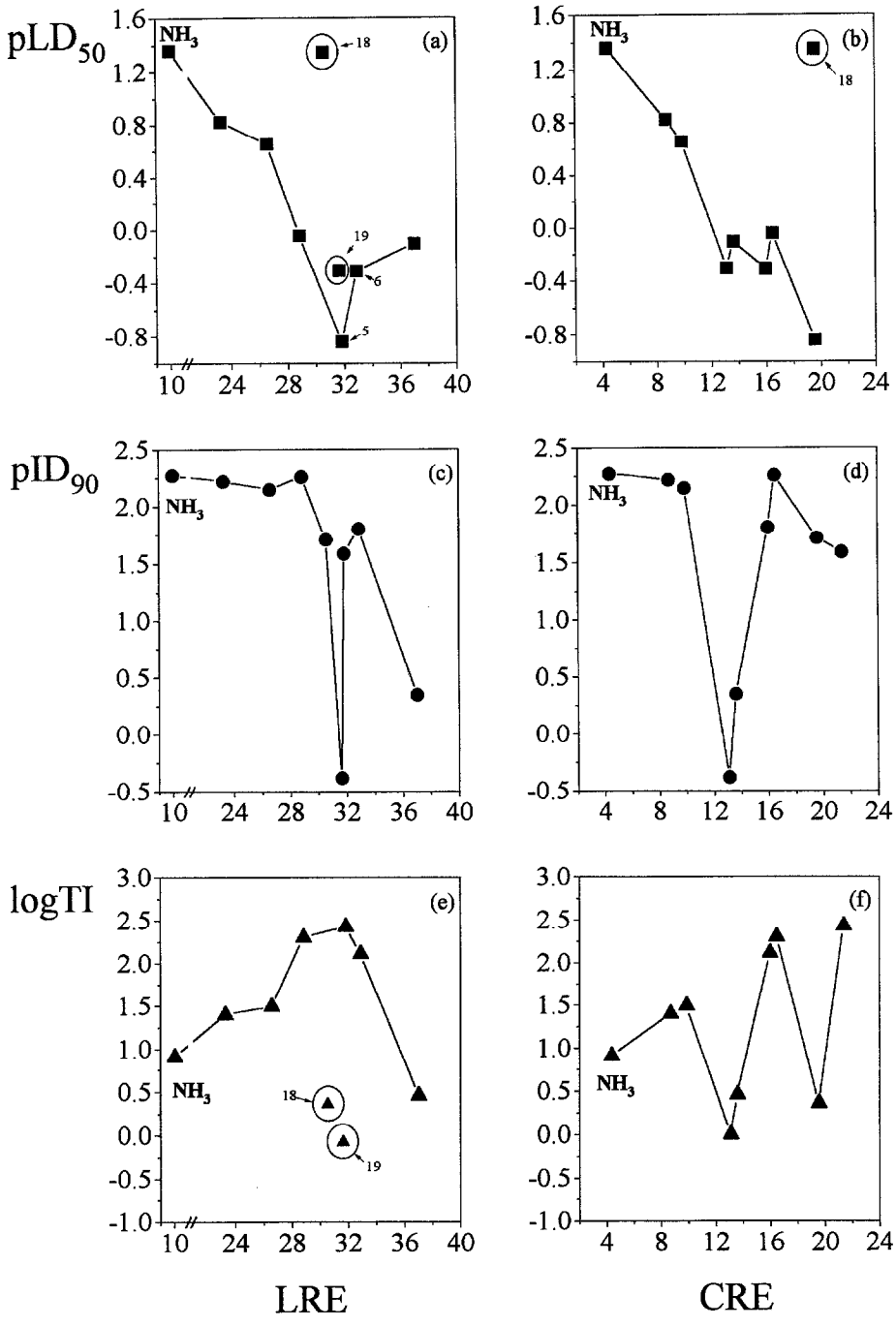

Fig. 8. Biological activity indicators versus steric descriptors LRE and CRE for cyclic systems.

(3) A degree of independence of biological activity with respect to electronic descriptors is suggested, at least for the amines under study. This is manifested by the vertical arrays of Fig. 6b. Notably, for all the electronic descriptors, the ligand NH_3 does not conform to this trend. The ligand cyclopropylamine also lies off the trend for a number of descriptors, namely $q(N)_{AM1}$, E_{LUMO}, ΔE and pK_a. Subsequent MLR analysis was carried out both with and without these two complexes and the results did not appear to be significantly different.

Collinearity

All structural descriptors used for the MLR analysis were checked for collinearity. The correlation matrix (Table 7) shows that the hydrophobicity does not correlate with any individual steric or electronic parameter used. For the two steric parameters, LRE correlates with two out of the six electronic parameters, although not strongly. The steric parameters LRE and CRE are not strongly correlated with one another, reflecting the different physical phenomena underlying their calculation. As

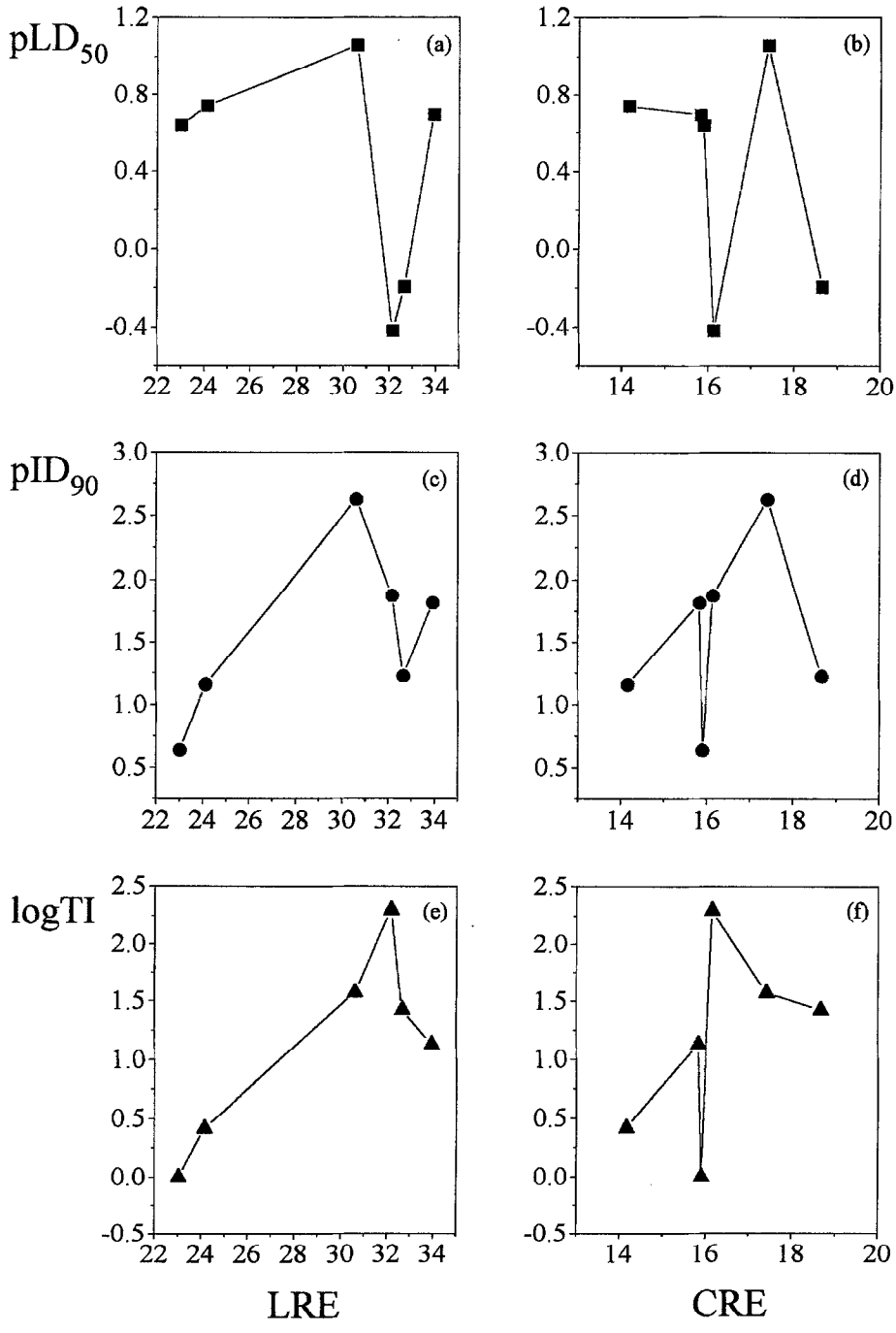

Fig. 9. Biological activity indicators versus steric descriptors LRE and CRE for branched-chain systems.

expected, electronic descriptors are strongly interrelated, except for pK_a.

Stepwise models

Table 8 (upper part) shows *stepwise* regression equations together with their goodness-of-fit (correlation strength), goodness-of-prediction and statistical significance parameters. The plots of the values of pLD_{50}, pID_{90} and log TI based on these equations are shown in Figs. 7a–c.

It appears from stepwise regression analysis that the biological activity of platinum complexes can be modelled quite well by carrier-ligand hydrophobicity. That is, the most significant factor influencing biological activity in this case appears to be transport, i.e. accumulation and distribution. However, it must be realised that factors which are operative at the target site may well be masked by transport effects. That is, the biological activity of a complex often depends on its ability to bind to target sites in a specific way, not simply to get there. This may

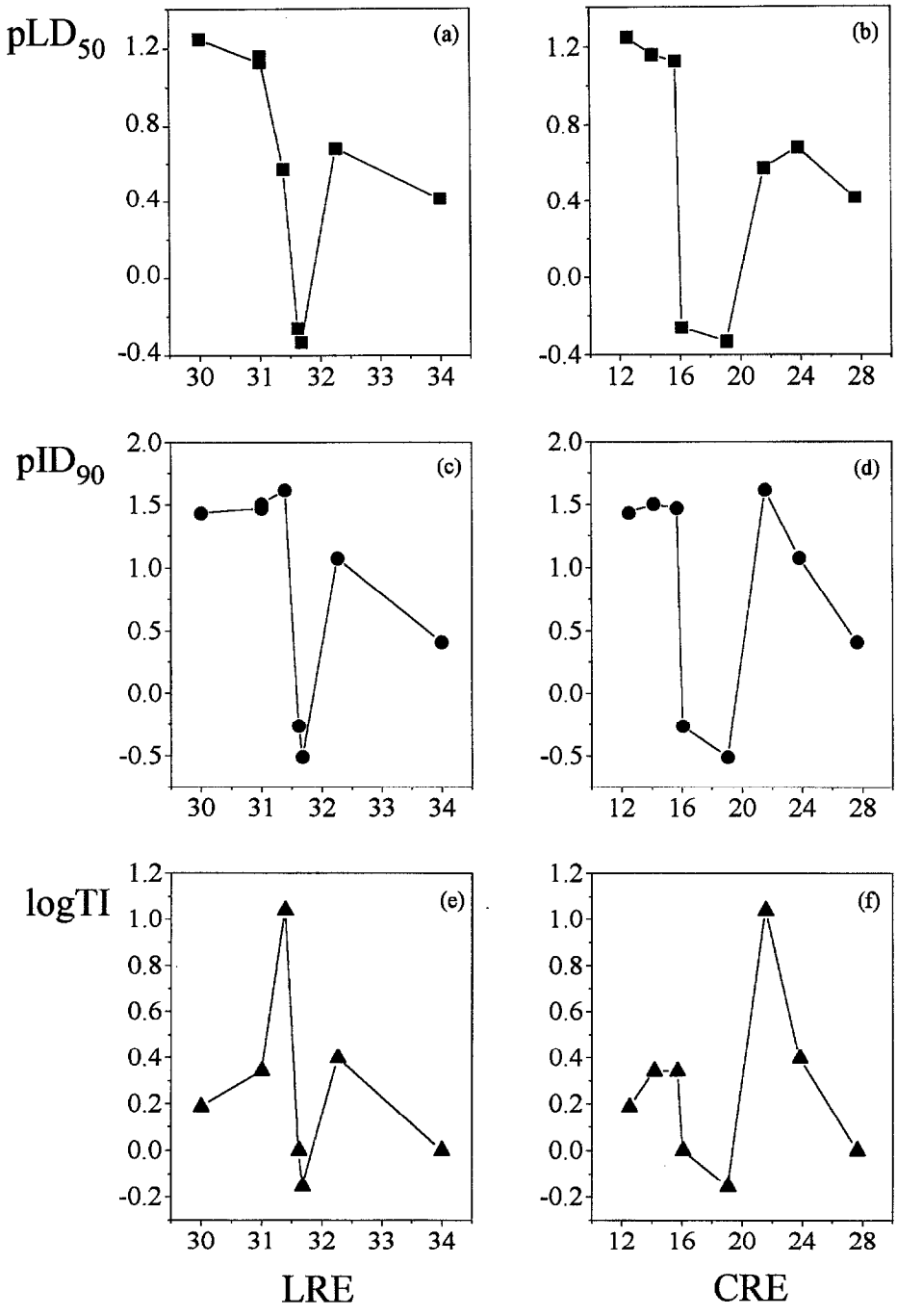

Fig. 10. Biological activity indicators versus steric descriptors LRE and CRE for straight-chain systems.

be accounted for by introducing second (and, if necessary, third) terms into the QSAR, in particular those that account for steric and/or electronic effects.

Enter models

Table 8 (middle and lower parts) show the 'best' *enter* regression equations together with their goodness-of-fit (correlation strength), goodness-of-prediction and statistical significance parameters. The plots of the values of pLD_{50}, pID_{90} and log TI based on these equations are shown in Figs. 7d–i, and show that the equations obtained are fairly predictive of toxicity and potency. The QSAR models for the therapeutic index, however, did not achieve the quality that was hoped for initially. A better choice of initial descriptors or a better formulation of the model (through different chemometric methods) is suggested.

The regression results presented here (using LRE and CRE as steric descriptors) show a marginal improvement (with respect to overall correlation strength and statistical

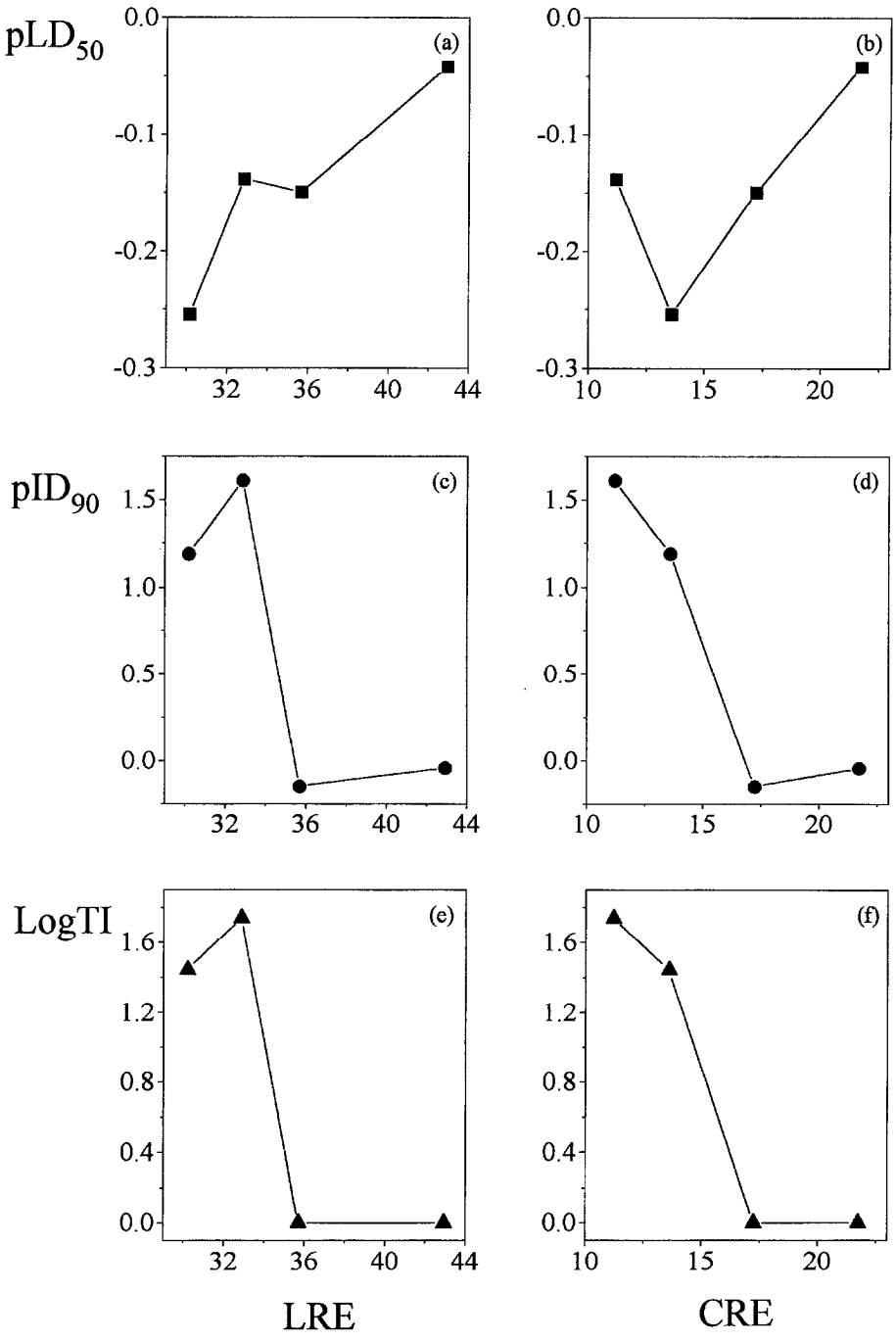

Fig. 11. Biological activity indicators versus steric descriptors LRE and CRE for polycyclic systems.

significance) in comparison with the *stepwise* models. However, the partial correlation coefficients and the statistical significance of variables describing steric and electronic effects are smaller than those of log P (data are not given here). In some cases these regression equations show an improvement in goodness-of-fit compared to those obtained in previous studies [4–9]; however, it is impossible to compare their predictive power since no cross-validation information is given in these works. In contrast to some previous studies [4,9], our results do not show a predominant dependency of biological activity on electronic structure. Rather, the importance of transport effects is emphasised. They also reveal a consistent contribution of steric effects to the biological outcomes.

Relationship of biological profiles with repulsive energies

Whilst it is acknowledged that the biological activity of platinum–am(m)ine complexes is dominated by their transport properties, reflected by a strong dependency on hydrophobicity as revealed by QSAR results (vide

infra), steric and electronic effects *after* the molecule has reached its target site may become determinative of their relative activities. We have attempted to extract further information on steric effects by looking for trends involving biological indicators and LRE and CRE within given series of ligands.

For example, the relationship between toxicity (pLD_{50}) and LRE is examined in Figs. 8a, 9a, 10a and 11a. It is apparent for cyclic (cycles), straight-chain (straights) and branched-chain (branches) systems that a pattern emerges. Interestingly, with increasing LRE, the toxicity tends to decrease to a minimum value of around 32 kcal/mol for each series and then rises again. This might be suggestive of an optimal steric requirement for minimum toxicity within a given series. Note that in Fig. 8a the circled data points representing ligands **18** (and possibly **19**) do not conform to the described trend. These ligands are characterised by having OH and CH_3 substituents in the 4-position of the ring. The remote location of these substituents from the donor amino group does not significantly influence their LRE values, as expected. Thus, **5**, **18** and **19** are in an approximately vertical array. It is interesting to note, however, that the absolute toxicity relating to ligand **18** is enhanced, which may be due to the additional hydrogen-bonding capability of the hydroxyl group, stabilising a drug–DNA adduct [44]. The absolute toxicity relating to ligand **19** is of the same order of magnitude as that for **6**; this is anticipated, considering that the hydrophobic character of both is very close. Complexes containing polycyclic ligands (polycycles) (Fig. 11a) can be considered as presenting only the 'right shoulder' of the above trend. This might be expected since there is a paucity of polycyclic hydrocarbons smaller than norbornane.

While toxicity versus LRE plots for individual series of compounds show that the toxicity passes through a minimum, the regression analysis with respect to toxicity for all compounds combined did not reveal a parabolic dependence on LRE. Thus, such trends appear to be series specific.

The relationship between the antitumour potency (pID_{90}) and LRE is shown in Figs. 8c, 9c, 10c and 11c, and reflects the trend observed for pLD_{50}. These trends could, perhaps, be exploited for ligands of these types for rational drug design. A full explanation of such patterns of behaviour is more difficult to address.

The relationship between therapeutic index (log TI) and LRE is shown in Figs. 8e, 9e, 10e and 11e. Plots of log TI versus LRE do not reveal any obvious pattern of behaviour. However, it is of interest to note that for cycles and branches, the ligand responsible for maximum log TI corresponds to the same ligand responsible for minimum pLD_{50}. This is not the case for straights and polycycles. In the case of straights it can be rationalised by the observation that they are less sterically diverse as a series (in terms of LRE), vide infra. Consequently, from a steric point of view, they do not differ significantly from each other and a variation in therapeutic index cannot be rationalised through steric effects. Series of platinum complexes with polycyclic amine ligands suffer from the lack of data. The availability of biological data for a wider range of polycyclic ligand complexes could probably lead to some rationale.

Biological profiles versus CRE (Figs. 8–11; b, d and f) show similar trends to those of LRE with some variations. In particular, for cycles the strongest repulsion between $Pt(NH_2R)_2Cl$ and 9-EtG corresponds to minimum toxicity, i.e. the optimal steric size of the ligand corresponds to minimum toxicity. But this trend is not general (as in e.g. straight chains). Presumably, other factors (both steric and nonsteric) contribute to toxicity and may predominate in some cases. However, as in the case of LRE, optimal values of CRE (15–20 kcal/mol) for minimum toxicity can be cautiously suggested. The variations between LRE and CRE trends are to be expected, since in $Pt(NH_2R)_2Cl$(9-EtG) systems the amine ligands are separated from the 'steric probe' by platinum. Furthermore, in these systems the repulsive contributions of two amine moieties are embedded into the calculations, and these two moieties are nonequivalent, one being cis to the N7 position and the other trans, see Fig. 2.

Conclusions

LRE and CRE parameters as applied to the approach of a metal complex to a target molecule allow for an improved description of steric effects in such systems. Where transport, electronic and steric effects are all to be considered, the LRE and CRE parameters have a higher degree of orthogonality than those employed previously. Future attempts to separate steric and transport effects and to expose purely steric requirement may include a consideration of steric effects in complexes containing ligands of like hydrophobicity. Other directions to investigate the scope of repulsive energy strategies for studying steric effects in biologically active metal complexes may well include quantitative structure–property relationship (QSPR) studies, allowing a focus on kinetic and/or thermodynamic properties. In addition, other chemometric techniques (e.g. PLS, PCA, neural nets [45]) may be more successful in finding a better QSAR/QSPR model in such systems, although our preliminary results show no improvement in goodness-of-fit and goodness-of-prediction in comparison with the results from MLR for the models, containing log P and CRE, log P and LRE, log P and pK_a, where some degree of collinearity is present. The repulsive energy strategy reported here is to be extended to other systems for which biological activity information is available, namely mixed and bidentate carrier ligands,

other possible targets on DNA, bisadducts and other biologically active metal complexes (e.g. Ref. 46).

Acknowledgements

We wish to thank Prof. Theodore L. Brown and Dr. David White of the University of Illinois at Urbana-Champaign for their advice and assistance. This research was supported in part by a Victoria University of Technology Postgraduate Research Scholarship (to E.Y.).

References

1 Barton, J.K., In Bertini, I., Gray, H.B., Lippard, S.J. and Valentine, J.S. (Eds.) Bioinorganic Chemistry, University Science Books, Mill Valley, CA, U.S.A., 1994, pp. 455–504.
2 Sherman, S.E. and Lippard, S.J., Chem. Rev., 87 (1987) 1153.
3 Braddock, P.D., Connors, T.A., Jones, M., Khokhar, A.R., Melzack, D.H. and Tobe, M.L., Chem.-Biol. Interact., 11 (1975) 145.
4 Abdul-Ahad, P.G. and Webb, G.A., Int. J. Quantum Chem., 21 (1982) 1105.
5 Simon, Z., Mracec, M., Maurer, A. and Policec, S., Rev. Roum. Chim., 25 (1980) 713.
6 Simon, Z., Holban, S., Mracec, M., Maurer, A., Policec, S. and Dragulescu, C., Rev. Roum. Biochim., 14 (1977) 117.
7 Romanowska, K. and Kudak-Jarowska, J., Arch. Immunol. Ther. Exp., 39 (1991) 75.
8 Romanowska, K., Int. J. Quantum Chem., 43 (1992) 175.
9 Tang, W., Qu, Y. and Dai, A., Pure Appl. Chem., 60 (1988) 1271.
10 Hansch, C., Venger, B.H. and Panthananickal, A., J. Med. Chem., 23 (1980) 459.
11 Hansch, C., Acc. Chem. Res., 26 (1993) 147. The public domain subset of the database can be reached at http://fox.pomona.claremont.edu/chem/qsar-db/index.html.
12 Quinn, F.R. and Milne, G.W.A., Fundam. Appl. Toxicol., 6 (1986) 270.
13 NCI Data, source a.panthananickal bio_1865. From Hansch, C., Acc. Chem. Res., 26 (1993) 147.
14 Charton, M., In Charton, M. and Motoc, I. (Eds.) Steric Effects in Drug Design, Springer, Berlin, Germany, 1983, pp. 107–118.
15 Motoc, I., In Charton, M. and Motoc, I. (Eds.) Steric Effects in Drug Design, Springer, Berlin, Germany, 1983, pp. 93-105.
16 Ghose, A.K. and Crippen, G.M., J. Med. Chem., 28 (1985) 333.
17 Hansch, C., In Chapman, N.B. and Shorter, J. (Eds.) Correlation Analysis in Chemistry, Plenum, New York, NY, U.S.A., 1978, pp. 397–438.
18 Bersuker, I.B. and Dimoglo, A.S., In Lipkowitz, K.B. and Boyd, D.B. (Eds.) Reviews in Computational Chemistry, Vol. 2, VCH, New York, NY, U.S.A., 1991, pp. 423–460.
19 Maliski, E.G. and Bradshaw, J., In Ganellin, C.R. and Roberts, S.M. (Eds.) Medicinal Chemistry. The Role of Organic Chemistry in Drug Research, Academic Press, London, U.K., 1993, pp. 83–102.
20 Belsley, D.A., Kuh, E. and Welsch, R.E., Regression Diagnostics: Identifying Influential Data and Sources of Collinearity, Wiley, New York, NY, U.S.A., 1980.
21 Tolman, C.A., Chem. Rev., 77 (1977) 313.
22 White, D., Taverner, B.C., Leach, P.G.L. and Coville, N.J., J. Comput. Chem., 14 (1993) 1042.
23 Choi, M.-G. and Brown, T.L., Inorg. Chem., 32 (1993) 1548.
24 Woo, T.K. and Ziegler, T., Inorg. Chem., 33 (1994) 1857.
25 Orbell, J.D., Marzilli, L.G. and Kistenmacher, T.J., J. Am. Chem. Soc., 103 (1981) 5126.
26 Orbell, J.D., Solorzano, C., Marzilli, L.G. and Kistenmacher, T.J., Inorg. Chem., 21 (1982) 3806.
27 Lippert, B., In Lippard, S.J. (Ed.) Progress in Inorganic Chemistry, Vol. 37, Wiley, New York, NY, U.S.A., 1989, pp. 2–97.
28 Silverman, R.B., The Organic Chemistry of Drug Design and Drug Action, Academic Press, San Diego, CA, U.S.A., 1992.
29 HyperChem is a commercial molecular modelling package from Hypercube Inc., Waterloo, ON, Canada. The MM+ force field of HyperChem is an extension of the MM2 code developed by N. Allinger. It uses the latest MM2 (1991) parameters with the 1977 functional form. HyperChem supplements the standard MM2 by providing additional parameters.
30 Gasteiger, J. and Marsili, M., Tetrahedron, 36 (1980) 3219.
31 Stewart, J.J.P., J. Comput.-Aided Mol. Design, 4 (1990) 1.
32 Klein, C.L. and Stevens, E.D., In Liebman, J.F. and Greenberg, A. (Eds.) Structure and Reactivity, VCH, New York, NY, U.S.A., 1988, pp. 25–64.
33 Fleming, I., Frontier Orbitals and Organic Chemistry Reactions, Wiley, Chichester, U.K., 1989.
34 Perrin, D.D., Dissociation Constants of Organic Bases in Aqueous Solutions, Butterworths, London, U.K., 1965.
35 Smith, R.M. and Martell, A.E., Critical Stability Constants, Plenum, New York, NY, U.S.A., 1975.
36 Perrin, D.D., Dempsey, B. and Serjeant, E.P., pK_a Prediction for Organic Acids and Bases, Chapman and Hall, London, U.K., 1981.
37 Ghose, A.K., Pritchett, A. and Gordon, M.C., J. Comput. Chem., 9 (1988) 80.
38 Yao, S., Plastaras, J.P. and Marzilli, L.G., Inorg. Chem., 33 (1994) 6061.
39 Nie, N.H., Bent, D.H. and Hull, C.H., Statistical Package for the Social Sciences, McGraw-Hill, New York, NY, U.S.A., 1970. Version 6.1 for Windows was used in this work.
40 SCAN, Software for Chemometric Analysis, 1995 by Minitab Inc. Release 1 for Windows was used in this work.
41 Plummer, E.L., In Lipkowitz, K.B. and Boyd, D.B. (Eds.) Reviews in Computational Chemistry, Vol. 1, VCH, New York, NY, U.S.A., 1990, pp. 119–168.
42 Choi, M.-G. and Brown, T.L., Inorg. Chem., 32 (1993) 5603.
43 Baker, A.T., Crass, J.K., Kok, G.B., Orbell, J.D. and Yuriev, E., Inorg. Chim. Acta, 214 (1993) 169.
44 Reedijk, J., Inorg. Chim. Acta, 198–200 (1992) 873.
45 Haswell, S.J. (Ed.) Practical Guide to Chemometrics, Marcel Dekker, New York, NY, U.S.A., 1992.
46 Kuo, L.Y., Kanatzidis, M.G., Sabat, M., Tipton, A.L. and Marks, T.J., J. Am. Chem. Soc., 113 (1991) 9027.